

## 4

# Lambert's Problem

### 4.1 Introduction

A fundamental problem in astrodynamics is the transfer of a spacecraft from one point in space to another. An example application is spacecraft targeting, in which the final point (the "target") is a planet or space station moving in a known orbit. In this situation, one might want the spacecraft to either *intercept* the target (match position only) or *rendezvous* with the target (match both position and velocity).

The initial point for an orbital rendezvous or interception is typically the location of the spacecraft in its orbit at the initial time. However, in other applications, such as ascent trajectories from the surface of the moon, the initial point can be at rest on the surface. Common to all orbit transfer applications is the determination of two-body orbits that connect specified initial and final points.

### 4.2 Transfer Orbits Between Specified Points

As shown in Fig. 4.1, consider points  $P_1$  and  $P_2$  described by radius vectors  $\mathbf{r}_1$  and  $\mathbf{r}_2$  relative to the focus  $F$  at the center of attraction. The end points  $P_1$  and  $P_2$  are separated by the transfer angle  $\theta$  and the chord  $c$ . The triangle  $FP_1P_2$  is sometimes referred to as the *space triangle* for the transfer.

First, let us investigate the possible transfer orbits between the specified endpoints  $P_1$  and  $P_2$ . For the case of elliptic transfer orbits, this can be accomplished using the simple geometric property shown in Fig. 4.2. A similar analysis can be done for parabolic and hyperbolic transfer orbits, but is not presented here.

The geometric property used is that the sum of the distances from any point on the ellipse to the focus and the vacant focus is a constant having value  $2a$ . This is the familiar property by which one can draw an ellipse by anchoring a piece of string at two points with thumbtacks, draw the string taut with the point of a pencil, and trace out an ellipse. In this mechanical device the thumbtacks locate the focus and vacant focus, and the string length is  $2a$ . Thus in Fig. 4.2

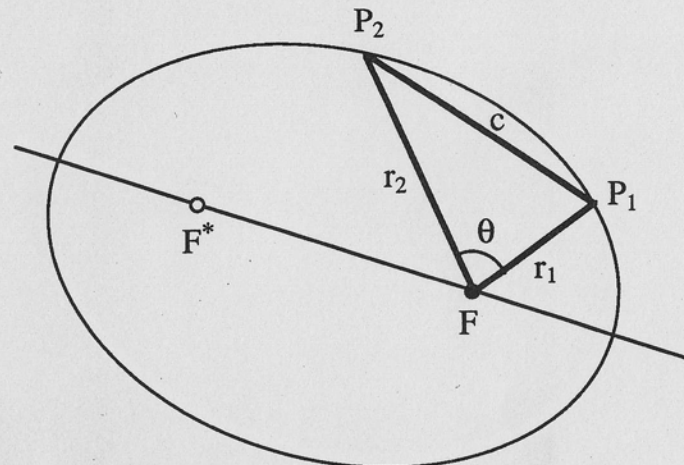


Fig. 4.1 Transfer Orbit Geometry

$$P_1F + P_1F^* = 2a \quad (4.1)$$

and

$$P_2F + P_2F^* = 2a$$

or

$$P_1F^* = 2a - r_1 \quad (4.2)$$

and

$$P_2F^* = 2a - r_2$$

For the remainder of the discussion, let us assume that  $r_2 \geq r_1$ , which implies no loss of generality, since the transfer orbit can be traversed in either direction. Because gravity is a conservative (nondissipative) force, one can determine the orbit that solves the boundary value problem in the reverse direction (starting at the final point  $P_2$  and ending at the initial point  $P_1$ ) by simply letting time run backward on the original orbit from  $P_2$  to  $P_1$ . This represents a valid forward time solution with the original velocity vector replaced by its negative.

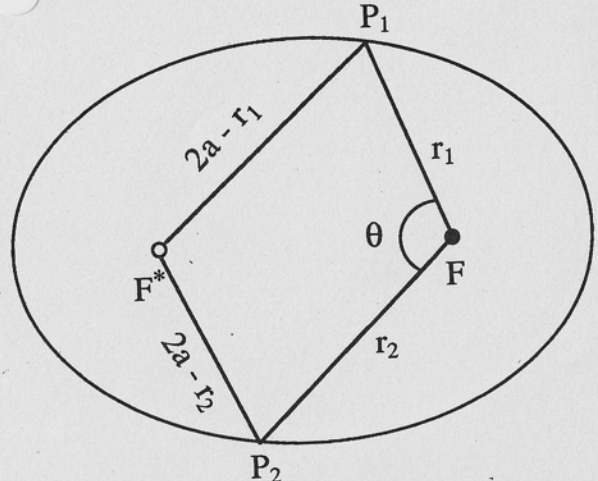


Fig. 4.2 A Geometric Property of Ellipses

For a given space triangle and specified value of semimajor axis  $a$ , Fig. 4.3 shows that a vacant focus is located at the intersection of two circles centered at  $P_1$  and  $P_2$  having respective radii  $2a - r_1$  and  $2a - r_2$  [Eq. (4.2)].

As shown in Fig. 4.3, the circular arcs for a given value of  $a = a_k$  intersect at two points labeled  $F_k^*$  and  $\tilde{F}_k^*$  that are equidistant from the chord  $c$ . This means that for the value of  $a$  depicted, there are two elliptic transfer orbits between  $P_1$  and  $P_2$ . As we will see, these two transfer orbits for the same value of  $a$  have different eccentricities and transfer times, but they have the same total energy.

From Fig. 4.3 it is evident that the distance  $FF^*$  is less than the distance  $FF\tilde{F}$ . Because the distance from the focus of an ellipse to the vacant focus is  $2ae$  (Sec. 1.5), this implies that the ellipse with vacant focus at  $F^*$  has the smaller eccentricity:  $e < \tilde{e}$ . Figure 4.4 shows the two elliptic transfer orbits for the case  $r_2 = 1.524 r_1$  (earth to Mars) with  $\theta = 107^\circ$  and a specified semimajor axis value of  $a = 1.36 r_1$ . The numerical values of the two eccentricities are  $e = 0.26$  and  $\tilde{e} = 0.68$  for this case.

Returning to Fig. 4.3 two other aspects of the problem are evident from the geometry. First, as the value of  $a$  is varied, the vacant foci describe a locus formed by the intersections of the circles of varying radii centered at  $P_1$  and  $P_2$ . This *locus of the focus* has the property that at any point on it the difference in the distances to the fixed points  $P_1$  and  $P_2$  is a constant, equal to  $r_2 - r_1$ . This implies that the locus itself (the solid line in Fig. 4.3) is a hyperbola with foci at  $P_1$  and  $P_2$ !

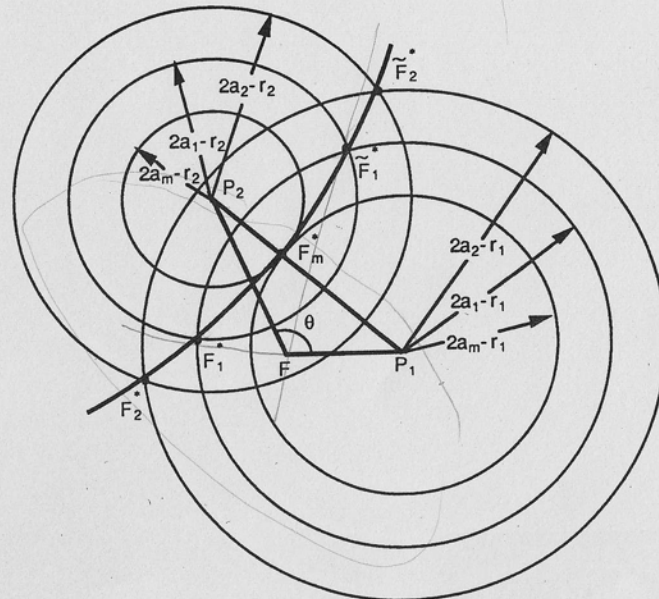


Fig. 4.3 Vacant Focus Locations

The second aspect of the problem that is evident from Fig. 4.3 is that as the value of  $a$  is decreased from the values shown, the two vacant foci approach the point  $F_m^*$  on the chord between  $P_1$  and  $P_2$ . For all values of  $a$  less than this value there is no intersection of the circles centered at  $P_1$  and  $P_2$ , which implies that no elliptic transfer connecting  $P_1$  and  $P_2$  exists for values of  $a$  less than a certain minimum value. This minimum value is denoted by  $a_m$  and its value is easily calculated from the geometry of the point  $F_m^*$  in Fig. 4.3:

$$(2a_m - r_2) + (2a_m - r_1) = c \quad (4.3)$$

or

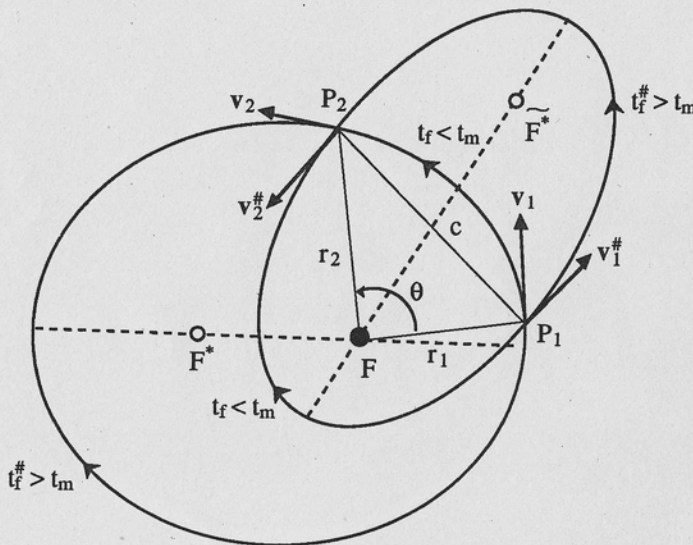
$$a_m = s/2 \quad (4.4)$$

where

$$s \equiv (r_1 + r_2 + c)/2 \quad (4.5)$$

## Earth - Mars Transfer

$$\begin{aligned}r_2 &= 1.524 r_1 \\.26 = e < e^* &= .68 \\ \theta &= 107^\circ \\ a &= 1.36 r_1 \\ a_m &= 1.14 r_1\end{aligned}$$

Fig. 4.4 Two Elliptic Transfer Orbits with the Same Value of  $a$ 

is the *semiperimeter* of the space triangle  $FP_1P_2$ .

In addition to describing the value of  $a_m$  geometrically, one can also interpret it dynamically by recalling that the value of  $a$  for a conic orbit is a measure of its total energy (Sec. 2.4). Thus the ellipse having semimajor axis  $a_m$  is the *minimum-energy ellipse* that connects the specified endpoints  $P_1$  and  $P_2$ . Orbit having a value of  $a$  less than  $a_m$  simply do not have enough energy at point  $P_1$  to reach point  $P_2$ . Some days are like that.

One other interesting geometric property of the elliptic transfer orbits between  $P_1$  and  $P_2$  concerns the eccentricities of these orbits. As will be shown, the locus of the eccentricity vectors is a straight line that is normal to the chord, as shown by Battin, Fill, and Shepperd in [4.1].

To demonstrate this, one uses the basic polar equation for a conic section

$$r = \frac{p}{1 + e \cos f} \quad (4.6)$$

to write

$$e \cdot r_1 = p - r_1; \quad e \cdot r_2 = p - r_2 \quad (4.7)$$

Subtracting and dividing by the chord  $c$  yields

$$-e \cdot (r_2 - r_1)/c = (r_2 - r_1)/c \quad (4.8)$$

Because  $(r_2 - r_1)/c$  is a unit vector along the chord directed from  $P_1$  to  $P_2$ , Eq. (4.8) implies that the eccentricity vectors for all the transfer orbits have a constant projection along the chord direction. This, in turn, implies that the locus of the eccentricity vectors is a straight line normal to the chord as shown in Fig. 4.5.

Also evident from Fig. 4.5 is the fact that there is a transfer ellipse of *minimum eccentricity*  $e_s$  whose value is simply [4.3]

$$e_s = \frac{r_2 - r_1}{c} \quad (4.9)$$

which is, interestingly, the reciprocal of the eccentricity of the hyperbolic locus of the vacant focus. This minimum eccentricity ellipse is also termed the *fundamental ellipse* because the point  $P_1$  has the same relationship to the occupied focus  $F$  as  $P_2$  does to the vacant focus  $F^*$ , due to the fact that the major axis of the ellipse is parallel to the chord.

## 4.3 Lambert's Theorem

A primary concern in orbit transfer is the transfer time, defined as the time required to travel from point  $P_1$  to point  $P_2$ . In the spacecraft targeting example mentioned earlier, the spacecraft is at point  $P_1$  in its orbit at a time  $t_1$  and the target will be at point  $P_2$  in its orbit at a later time  $t_2$ . The transfer time is then  $t_2 - t_1$  and the crucial issue is the determination of the transfer orbit that connects the specified endpoints in the given transfer time. Because of the work of Johann Heinrich Lambert (1728–1779), this is often called *Lambert's problem*.

The theorem which bears his name is due to his conjecture in 1761, based on geometric reasoning, that the time required to traverse an elliptic arc between specified endpoints depends only on the semimajor axis of the ellipse, and on two geometric properties of the space triangle, namely the chord length and the sum of the radii from the focus to points  $P_1$  and  $P_2$ :

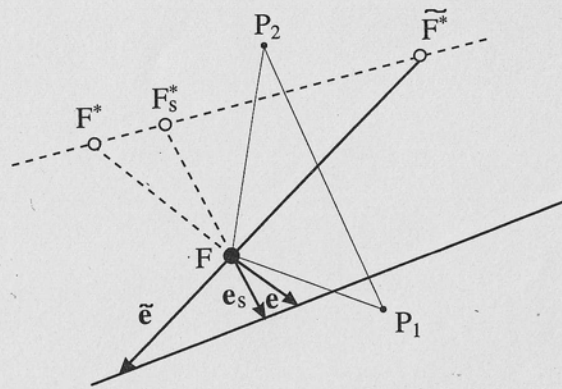


Fig. 4.5 Locus of Eccentricity Vectors

$$t_2 - t_1 = f(a, c, r_1 + r_2) \quad (4.10)$$

This result was actually first obtained analytically by Lagrange in 1778, one year before Lambert's death.

This is the third instance encountered of an important property of elliptic orbits that depends on the semimajor axis but is independent of the eccentricity. The other two are the period of an elliptic orbit and the total energy of the orbit (i.e. the velocity as a function of the radius given by the vis-viva equation).

In order to derive an equation describing the transfer time, we make use of our previously obtained equation relating time and position, namely Kepler's equation. The essential difference here is that Lambert's problem is an orbital *boundary value problem*, whereas Kepler's equation describes an *initial value problem*. If one lets  $E_2$  and  $E_1$  denote the (unknown) values of eccentric anomaly at times  $t_2$  and  $t_1$  on the transfer ellipse, Kepler's equation yields:

$$\sqrt{\mu} (t_2 - t_1) = a^{3/2} [E_2 - E_1 - e (\sin E_2 - \sin E_1)] \quad (4.11)$$

This form is not very convenient for the boundary value problem because both  $a$  and  $e$  of the transfer orbit are unknown (to be determined) and because, according to Lambert's theorem, the transfer time does not actually depend on the value of  $e$ . In order to get the transfer time equation into a

more convenient form, define

$$E_P = \frac{1}{2} (E_2 + E_1)$$

and

$$E_M = \frac{1}{2} (E_2 - E_1) > 0 \quad (4.12)$$

Using the fact that  $r = a(1 - e \cos E)$ ,

$$r_1 + r_2 = a[2 - e(\cos E_1 + \cos E_2)] \quad (4.13)$$

$$= 2a[1 - e \cos E_P \cos E_M] \quad (4.14)$$

In terms of cartesian coordinates with origin at the geometric center of the ellipse with the  $x$ -axis along the major axis (see Fig. 2.1):

$$x = a \cos E \quad (4.15)$$

$$y = b \sin E ; \quad b = a(1 - e^2)^{1/2} \quad (4.16)$$

and the chord distance can be obtained from

$$\begin{aligned} c^2 &= (x_2 - x_1)^2 + (y_2 - y_1)^2 \\ &= a^2[(\cos E_2 - \cos E_1)^2 + (1 - e^2)(\sin E_2 - \sin E_1)^2] \\ &= 4a^2 \sin^2 E_M (1 - e^2 \cos^2 E_P) \end{aligned} \quad (4.17)$$

The temptation is irresistible to let

$$\cos \xi = e \cos E_P \quad (4.18)$$

which is allowable only because the numerical value of  $e$  does not exceed unity. This leads to a perfect square on the right-hand side of Eq. (4.17), resulting in

$$c = 2a \sin E_M \sin \xi \quad (4.19)$$

Equation (4.14) can then be rewritten as

$$r_1 + r_2 = 2a(1 - \cos E_M \cos \xi) \quad (4.20)$$

Finally, let

$$\alpha = \xi + E_M \quad (4.21a)$$

$$\beta = \xi - E_M \quad (4.21b)$$

Now one can combine Eqs. (4.19), (4.20), and (4.21) to write:

$$r_1 + r_2 + c = 2a(1 - \cos \alpha) = 4a \sin^2(\alpha/2) \quad (4.22)$$

$$r_1 + r_2 - c = 2a(1 - \cos \beta) = 4a \sin^2(\beta/2) \quad (4.23)$$

Equation (4.11) for the transfer time becomes

$$\sqrt{\mu}(t_2 - t_1) = 2a^{3/2}(E_M - \cos \xi \sin E_M) \quad (4.24)$$

whence our final result is

$$\sqrt{\mu}(t_2 - t_1) = a^{3/2}[\alpha - \beta - (\sin \alpha - \sin \beta)] \quad (4.25)$$

To summarize, Eq. (4.25), sometimes called *Lambert's equation*, describes the elliptic transfer time  $t_2 - t_1$  for the case of less than one complete revolution  $0 \leq \theta < 2\pi$ , where the variables  $\alpha$  and  $\beta$  are determined from Eqs. (4.22) and (4.23) as

$$\sin\left(\frac{\alpha}{2}\right) = \left(\frac{s}{2a}\right)^{1/2} \quad (4.26)$$

$$\sin\left(\frac{\beta}{2}\right) = \left(\frac{s - c}{2a}\right)^{1/2} \quad (4.27)$$

As defined before,  $s$  is the semiperimeter of the space triangle, equal to  $\frac{1}{2}(r_1 + r_2 + c)$ . Note that Lambert's theorem as stated in Eq. (4.10) has been proved, since the angles  $\alpha$  and  $\beta$  depend only on  $a$ ,  $c$ , and  $r_1 + r_2$ .

#### 4.4 Properties of the Solutions to Lambert's Equation

Equation (4.25) must provide the solutions for the transfer times on all elliptic arcs of less than one revolution that connect points  $P_1$  and  $P_2$  for a given space triangle and a specified value for  $a$ . Returning to Fig. 4.4, it can be seen that for  $a > a_m$  there are four such arcs. (Recall that the direction of traversal on these arcs is irrelevant to the analysis because time-reversed solutions are valid as forward time solutions.) Two of these arcs have a transfer angle  $\theta < \pi$  as shown; the other two correspond to a transfer angle greater than  $\pi$ , and are formed by the remaining portions of the ellipses containing the smaller transfer angle arcs.

These four solutions for the transfer time correspond to quadrant ambiguities associated with the angles  $\alpha$  and  $\beta$ . The principal values of the inverse sine function used to solve Eqs. (4.26) and (4.27) yield angles  $\alpha_0$  and

$\beta_0$  characterized by  $0 \leq \beta_0 \leq \alpha_0 \leq \pi$ . In order to determine which one of the four arcs corresponds to these principal values and what quadrant corrections are needed for the other arcs, it is convenient to utilize the geometric interpretation of the angles  $\alpha$  and  $\beta$  derived by Prussing [4.2].

The derivation of the geometric interpretation is based on two properties of elliptic motion: (1) the transfer time must satisfy Kepler's equation, and (2) the shape of the transfer orbit can be altered by moving the focus  $F$  and the vacant focus  $F^*$  without altering the transfer time or the angles  $\alpha$  and  $\beta$  as long as  $r_1 + r_2$ ,  $c$ , and  $a$  remain unchanged. Using this property the focus and vacant focus can be moved to the locations  $F_R$  and  $F_R^*$  shown in Fig. 4.6, which define a *rectilinear elliptic orbit* ( $e = 1$ ,  $p = 0$ ) between points  $P_1$  and  $P_2$ . This rectilinear orbit has the same values of  $r_1 + r_2$ ,  $c$ , and  $a$  and hence the same transfer time,  $\alpha$  and  $\beta$  as the original orbit.

Kepler's equation for the transfer time between two points in an elliptic orbit whose locations are specified by the values of eccentric anomaly  $E$  is

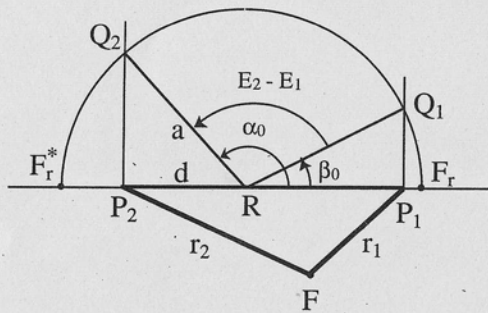
$$\sqrt{\mu}(t_2 - t_1) = a^{3/2}[E_2 - E_1 - e(\sin E_2 - \sin E_1)] \quad (4.28)$$

By comparing Eq. (4.28) with (4.25), one can interpret the angles  $\alpha$  and  $\beta$  as the values of eccentric anomaly on the rectilinear ellipse between  $P_1$  and  $P_2$  having the same value of  $a$ ,  $c$ , and  $r_1 + r_2$ .

The geometric interpretation of  $\alpha$  and  $\beta$  and the quadrants for these angles then follows the classical geometric interpretation of eccentric anomaly encountered previously (Sec. 2.2). As shown in Fig. 4.6, one constructs the auxiliary circle of radius  $a$  centered at the center  $R$  of the rectilinear ellipse, located a distance  $d = s - a$  from  $P_2$ . Points  $Q_1$  and  $Q_2$  are the intersections of lines normal to the chord through  $P_1$  and  $P_2$  with the auxiliary circle. The principal value angles  $\alpha_0$  and  $\beta_0$  are shown in Fig. 4.6. Also shown is the fact that the difference  $\alpha - \beta$  (regardless of quadrant) is equal to the difference in the values of eccentric anomaly on the *original* elliptic path between points  $P_1$  and  $P_2$  [see Eq. (4.21)].

Figure 4.7 shows separately the four elliptic arcs originally shown in Fig. 4.4, along with the corresponding geometric interpretations of the angles  $\alpha$  and  $\beta$ . The top two figures depict the case  $\theta \leq \pi$  and are characterized by  $\beta = \beta_0 \leq \pi$ . The top figure corresponds to the shorter transfer time for the given transfer angle for which  $\alpha = \alpha_0 \leq \pi$ . The second figure corresponds to the longer transfer time, for which  $\alpha = 2\pi - \alpha_0 \geq \pi$ .

For a given transfer angle the behavior of the transfer time  $t_2 - t_1$  as a function of semimajor axis is shown in Fig. 4.8. For  $a > a_m$  the two elliptic arcs are characterized by one having a transfer time *defined as*  $t_F$ , which is less than  $t_m$ , the time on the minimum energy arc. The other has a transfer time *defined as*  $t_F^\#$ , which is greater than  $t_m$ . The value of  $t_m$  is easily

Fig. 4.6 Interpretations of Angles  $\alpha_0$  and  $\beta_0$ 

determined from Eq. (4.25) using the fact that  $a_m = s/2$  [Eq. (4.4)]. Equations (4.26) and (4.27) then tell us that

$$\alpha_m = \pi, \quad \sin(\beta_m/2) = \left[ \frac{s-c}{s} \right]^{1/2} \quad (4.29)$$

and the time is given by

$$\sqrt{\mu} t_m = \left( \frac{s^3}{8} \right)^{1/2} (\pi - \beta_m + \sin \beta_m) \quad (4.30)$$

where for  $0 \leq \theta \leq \pi$ ,  $\beta_m = \beta_{m0}$ , and for  $\pi \leq \theta \leq 2\pi$ ,  $\beta_m = -\beta_{m0}$ . The limiting value of transfer time along the lower part of the curve of Fig. 4.8 is the *parabolic transfer time*  $t_p$ , which is approached asymptotically as  $a \rightarrow \infty$ . This will be discussed in more detail shortly.

Returning to Fig. 4.7, the lower two figures correspond to  $\theta \geq \pi$  for which  $\beta = -\beta_0$  with  $\alpha = \alpha_0$  on the shorter transfer time arc and  $\alpha = 2\pi - \alpha_0$  on the longer time arc.

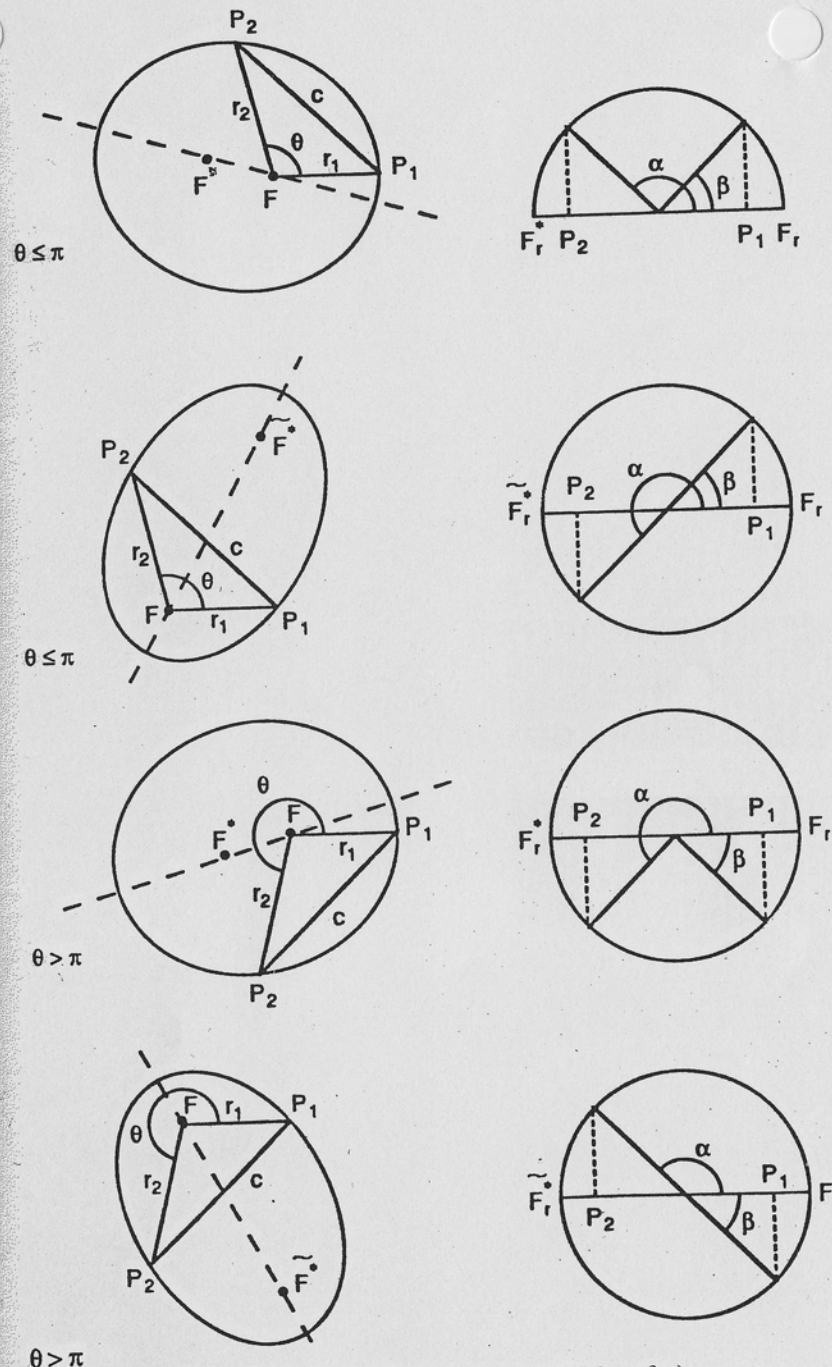
To summarize, a single equation (4.25) can be used for all elliptic arcs with  $0 \leq \theta < 2\pi$ , with the values of  $\alpha$  and  $\beta$  determined from the principal values  $0 \leq \beta_0 \leq \alpha_0 \leq \pi$  as follows:

$$0 \leq \theta < \pi, \quad \beta = \beta_0 \quad (4.31a)$$

$$\pi \leq \theta < 2\pi, \quad \beta = -\beta_0 \quad (4.31b)$$

$$t_2 - t_1 = t_F \leq t_m, \quad \alpha = \alpha_0 \quad (4.32a)$$

$$t_2 - t_1 = t_F^\# > t_m, \quad \alpha = 2\pi - \alpha_0 \quad (4.32b)$$

Fig. 4.7 The Four Elliptic Arcs (Same Value of  $a$ )

Note that for the special case  $\theta = \pi$ ,  $s = c$  and  $\beta_0 = 0$ ; therefore,  $\beta$  is continuous at  $\theta = \pi$ . Also, for  $t_2 - t_1 = t_m$ , as mentioned in Eq. (4.29)  $\alpha_0 = \pi$ , and  $\alpha$  is continuous at the transfer time  $t_m$ .

The equation describing the parabolic transfer time between specified endpoints is called *Euler's equation* (not that Euler needs another equation named after him) because this special case was published by Euler in 1743, almost 20 years before Lambert's more general result. It can be obtained by carefully taking the limit of the Lambert equation for an elliptic orbit as  $a \rightarrow \infty$  (Prob. 4.3). The result can be compactly written using the *signum function*,  $\text{sgn}$ , defined by

$$\text{sgn}(x) = \begin{cases} 1 & \text{for } x > 0 \\ -1 & \text{for } x < 0 \end{cases} \quad (4.33)$$

Euler's equation is then

$$\sqrt{\mu} (t_2 - t_1) = \sqrt{\mu} t_p = \frac{\sqrt{2}}{3} [s^{3/2} - \text{sgn}(\sin \theta) (s - c)^{3/2}] \quad (4.34)$$

where the term  $\text{sgn}(\sin \theta)$  automatically accounts for the required sign change going from transfer angles less than  $\pi$  to greater than  $\pi$ . This equation yields a value of  $t_p = 72$  days for the earth-Mars transfer geometry in Fig. 4.8. The value of  $t_p$  is important, since for an elliptic transfer to exist between specified endpoints, the transfer time must be greater than  $t_p$ .

A universal formulation of Lambert's equation exists using the special functions  $S$  and  $C$  described in Chap. 2. The Battin-Vaughan algorithm [4.4] and the Gooding procedure [4.5] are excellent methods for the iterative solution to Lambert's equation for the transfer orbit given the transfer time, is based on universal variables. This application is discussed in more detail in Sec. 4.6. A complete analysis of Lambert's problem in universal variables is given in [4.3].

#### Example 4.1

Consider the example transfer depicted in Fig. 4.8 with  $r_1 = 1$  au,  $r_2 = 1.524$  au, and  $\theta = 75^\circ$ . The terminal radii represent an earth-Mars transfer orbit. For this geometry the chord  $c = 1.592$  au, and the semiperimeter  $s = 2.058$  au. From Eq. (4.4) the value of  $a_m$  is determined to be 1.03 au, as shown in Fig. 4.8. From Eqs. (4.29) and (4.30) this yields a value of time on the minimum energy ellipse of  $t_m = 3.117$  canonical time units ( $\mu = 1$ ) that corresponds to 181 days.

For a transfer time  $t_2 - t_1$  equal to 115 days = 1.978 time units, Eq. (4.25) can be solved (by numerical iteration) for the value of  $a$ . Because the value of  $\theta$  is less than  $180^\circ$ ,  $\beta$  is simply  $\beta_0$  as indicated in Eq. (4.31a). Also,

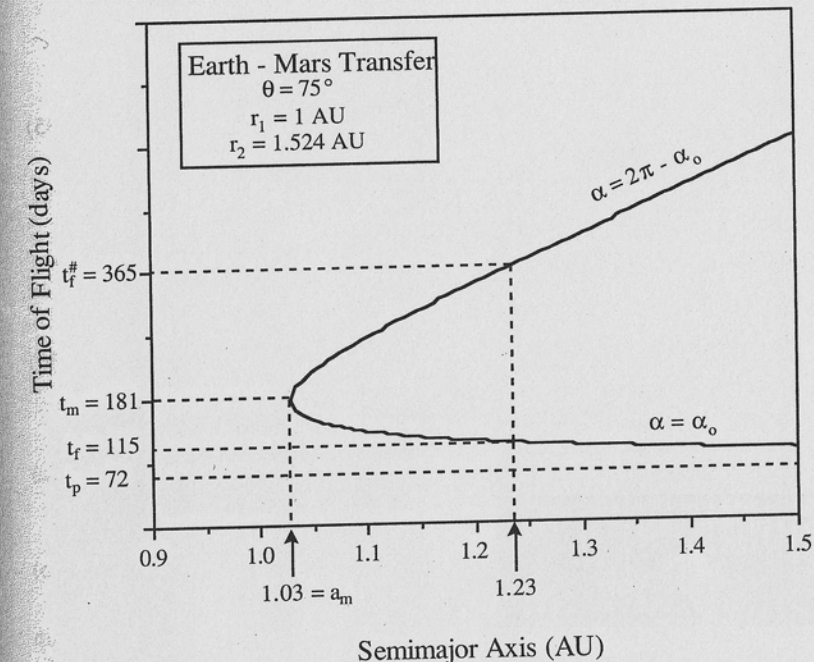


Fig. 4.8 Transfer Time vs. Semimajor Axis

because the specified transfer time is less than  $t_m$ , the solution for  $a$  lies on the lower portion of the curve in Fig. 4.8, and the specified time is denoted by  $t_F$ . The value of  $\alpha$  that applies in this case is simply  $\alpha_0$  as indicated in Eq. (4.32a). The value of  $a$  obtained is 1.232 au, which corresponds to  $\alpha_0 = 2.305 = 132.1^\circ$  and  $\beta_0 = 0.900 = 51.6^\circ$ . Thus the unique value of  $a$  has been determined for the specified transfer time.

The other value of transfer time for this same value of  $a$  lies on the upper portion of the curve in Fig. 4.8, corresponding to the transfer time  $t_F^*$ . To determine this value,  $\alpha = 2\pi - \alpha_0$  in Eq. (4.25), as indicated in Eq. (4.32b). The value obtained is  $t_F^* = 6.279$  time units = 365 days.

#### 4.5 The Terminal Velocity Vectors

The terminal velocity vectors  $v_1$  at  $r_1$  and  $v_2$  at  $r_2$  can be conveniently expressed in terms of a set of skewed unit vectors, one along the *local radius*

vector and the other along the chord. Specifically, let

$$\begin{aligned} \mathbf{u}_1 &\equiv \frac{\mathbf{r}_1}{r_1} \\ \mathbf{u}_2 &\equiv \frac{\mathbf{r}_2}{r_2} \\ \mathbf{u}_c &\equiv \frac{(\mathbf{r}_2 - \mathbf{r}_1)}{c} \end{aligned} \quad (4.35)$$

as shown in Fig. 4.9.

It can be shown that the velocity vector  $\mathbf{v}_1$  can be expressed as

$$\mathbf{v}_1 = (B + A) \mathbf{u}_c + (B - A) \mathbf{u}_1 \quad (4.36)$$

where

$$A = \left[ \frac{\mu}{4a} \right]^{\frac{1}{2}} \cot \left( \frac{\alpha}{2} \right) \quad (4.37a)$$

$$B = \left[ \frac{\mu}{4a} \right]^{\frac{1}{2}} \cot \left( \frac{\beta}{2} \right) \quad (4.37b)$$

with the values of  $\alpha$  and  $\beta$  being determined from Eqs. (4.26) and (4.27) with quadrant modifications given by Eqs. (4.31) and (4.32).

Equation (4.36) can be used to determine the terminal velocity vectors  $\mathbf{v}_1$  and  $\mathbf{v}_2$  for all the transfer ellipses having a given value of semimajor axis  $a$ . For specified values of the transfer angle  $\theta \leq \pi$  and semimajor axis  $a$ , the principal values  $\alpha_0$  and  $\beta_0$  in Eqs. (4.37) yield the correct components of  $\mathbf{v}_1$  for the case  $t_2 - t_1 = t_F < t_m$ . The initial velocity  $\mathbf{v}_1^*$  on the other transfer ellipse having the same value of  $a$ , but with  $t_2 - t_1 = t_F^* > t_m$  is obtained by using  $\alpha = 2\pi - \alpha_0$  in Eq. (4.37). This has the effect of merely changing the algebraic sign of the coefficient  $A$  in Eq. (4.36). This change in sign is equivalent to interchanging the chordal and radial components of the velocity vector in Eq. (4.36). Thus, the components of  $\mathbf{v}_1^*$  are easily obtained from the components of  $\mathbf{v}_1$ , and, because the value for  $a$  is the same for both,  $|\mathbf{v}_1| = |\mathbf{v}_1^*|$  (see Fig. 4.4).

The components of the final velocity  $\mathbf{v}_2$  at  $\mathbf{r}_2$  can also be obtained using Eq. (4.36) by considering a transfer backward in time from  $P_2$  to  $P_1$ . In this context the velocity vector  $-\mathbf{v}_2$  is the "initial" velocity, the chordal unit vector toward the final point is  $-\mathbf{u}_c$ , and the "initial" radial unit vector is  $\mathbf{u}_2$ . Equation (4.36) then becomes:

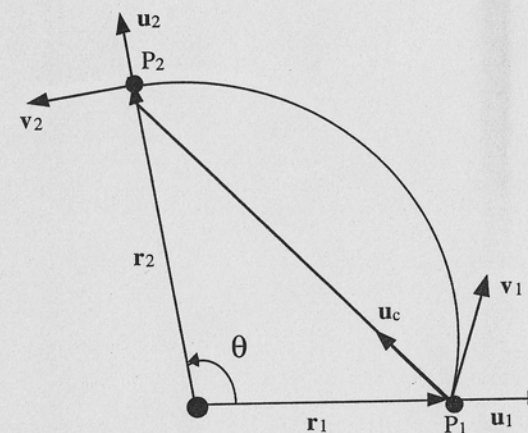


Fig. 4.9 Unit Vector Definitions

$$-\mathbf{v}_2 = (B + A)(-\mathbf{u}_c) + (B - A) \mathbf{u}_2 \quad (4.38)$$

or,

$$\mathbf{v}_2 = (B + A) \mathbf{u}_c - (B - A) \mathbf{u}_2 \quad (4.39)$$

Comparing Eqs. (4.36) and (4.39), one can see that the chordal components of the terminal velocities  $\mathbf{v}_1$  and  $\mathbf{v}_2$  are equal, whereas the local radial components are the negatives of each other.

Finally, the terminal velocities on the transfer ellipse for which  $\pi < \theta < 2\pi$  are obtained by changing the sign on  $\beta$ , as in Eq. (4.31). This has the effect of changing the sign of the coefficient  $B$  in Eq. (4.36), which is equivalent to replacing the chordal component by the negative of the local radial components, and vice-versa. This makes sense, because the velocity vectors for  $\theta > \pi$  and transfer time  $t_F$  are simply the negatives of the velocity vectors for  $\theta < \pi$  and transfer time  $t_F^*$  (see Fig. 4.4).

In the typical application, for which the transfer angle  $\theta$  and the transfer time  $t_2 - t_1$  are specified, the transfer ellipse and the corresponding terminal velocity vectors are unique. The appropriate values of  $\alpha$  and  $\beta$  must

be used to obtain the correct orbit and the terminal velocities.

It should be noted that for  $\theta = \pi$  Eq. (4.36) is indeterminant because the chordal unit vector and the local radial unit vectors become parallel. In this case, an alternate form of the velocity vector equation must be used.

#### Example 4.2

The velocity vectors corresponding to the transfer shown in Fig. 4.8 utilize the unit vectors:  $\mathbf{u}_1^T = [1 \ 0 \ 0]$ ,  $\mathbf{u}_2^T = [0.2588 \ 0.9659 \ 0]$ , and  $\mathbf{u}_c^T = [-0.3804 \ 0.9248 \ 0]$ , which yields, using Eqs. (4.36) and (4.39):

$$\mathbf{v}_1^T = [0.3015 \ 1.0476 \ 0] ; \mathbf{v}_2^T = [-0.6205 \ 0.3401 \ 0]$$

While not a direct result from the Lambert problem, it can be noted that the universal variable  $x$  at point  $P_1$  is, of course, 0, and the value at point  $P_2$  is determined from the universal Kepler's Eq. (2.39) to be  $x = 1.5609$ .

#### 4.6 Applications of Lambert's Equation

The typical application of Lambert's Eq. (4.25) is to determine the orbit and the terminal velocity vectors for specified  $\mathbf{r}_1$ ,  $\mathbf{r}_2$ , and  $t_2 - t_1$ . The procedure is as follows:

1. Calculate the parabolic transfer time  $t_p$  using Eq. (4.34). If the specified  $t_2 - t_1 > t_p$ , an elliptic transfer orbit exists. Otherwise the orbit must be parabolic or hyperbolic.
2. Calculate  $t_m$  using Eq. (4.30) and note whether  $t_2 - t_1$  is greater than or less than  $t_m$ . This determines the correct value of  $\alpha$  in Eq. (4.32). The correct value of  $\beta$  is determined by the value of the transfer angle  $\theta$  through Eq. (4.31).
3. Iteratively solve Lambert's Eq. (4.25) for the unique value of semimajor axis  $a$ . Standard iteration algorithms can be used, but the powerful universal algorithms developed by Battin and Vaughan [4.4] and Gooding [4.5] are recommended.
4. Once the value of  $a$  is determined, the terminal velocity vectors can be determined using Eq. (4.36) as discussed in Sec. 4.5.

The value of the eccentricity of the transfer orbit is best determined by first obtaining the parameter:

$$p = \frac{4a(s - r_1)(s - r_2)}{c^2} \sin^2 \left[ \frac{\alpha + \beta}{2} \right] \quad (4.40)$$

where  $\alpha$  and  $\beta$  are determined as before by Eqs. (4.31) and (4.32). Then  $e$  can be determined from  $a$  and  $p$  using  $p = a(1 - e^2)$ .

One further aspect of the application is the possibility of long-duration arcs for which the transfer time is long enough so that multiple revolution solutions exist, for which  $\theta \geq 2\pi$ . In this case the transfer orbit is nonunique. One can always find a transfer of sufficiently large  $a$  that  $\theta < 2\pi$  for the given transfer time, but there are a total of  $2N + 1$  distinct solutions if the transfer time is long enough to allow  $N$  complete revolutions of the focus, where  $2N\pi \leq \theta < (N + 1)\pi$ . The transfer time for  $N \geq 1$  is related to the transfer time for  $N = 0$  [Eq. (4.25)] by simply adding the term  $NT$ , where  $T$  is the period of the transfer orbit [Eq. (1.41)]:

$$\sqrt{\mu}(t_2 - t_1) = a^{3/2} [2N\pi + \alpha - \beta - (\sin \alpha - \sin \beta)] \quad (4.41)$$

#### References

- 4.1 Battin, R. H., Fill, T. J., and Shepperd, S. W., "A New Transformation Invariant in the Orbital Boundary-Value Problem," *Journal of Guidance and Control*, 1, 1, Jan-Feb. 1978, pp. 50-55.
- 4.2 Prussing, J. E., "A Geometrical Interpretation of the Angles Alpha and Beta in Lambert's Problem," *Journal of Guidance and Control*, 2, 5, Sept-Oct. 1979, pp. 442-443.
- 4.3 Battin, R. H., *An Introduction to the Mathematics and Methods of Astrodynamics*, American Institute of Aeronautics and Astronautics, New York, 1987.
- 4.4 Battin, R. H., and Vaughan, R. M., "An Elegant Lambert Algorithm," *Journal of Guidance, Control and Dynamics*, 7, 6, Nov-Dec. 1984, pp. 662-670.
- 4.5 Gooding, R. H., "A Procedure for the Solution of Lambert's Orbital Value Problem," *Celestial Mechanics*, 48, 1990, pp. 145-165.

#### Problems

- 4.1 a) For a given space triangle, determine expressions for the terminal velocity vectors  $\mathbf{v}_{1m}$  and  $\mathbf{v}_{2m}$  on the minimum energy orbit between  $P_1$  and  $P_2$  in terms of the unit vectors  $\mathbf{u}_c$ ,  $\mathbf{u}_1$ , and  $\mathbf{u}_2$ .  
b) Interpret the directions of these velocity vectors geometrically in terms of the unit vector directions.
- 4.2 Consider the earth and Jupiter to be in coplanar circular orbits of radii 1 au and 5.2 au, respectively.  
a) Considering the transfer angle  $\theta$  as a variable, determine the range

of values of  $a_m$  for all the possible earth-Jupiter transfer ellipses.  
 b) For  $\theta = 150^\circ$  and  $a = 5$  au, calculate the values of  $a_m$  (in au),  $t_m$ ,  $t_F$ ,  $t_F^{\#}$ , and  $t_p$  (in years).  
 c) Calculate  $\mathbf{v}_1$  and  $\mathbf{v}_1^{\#}$  (in EMOS) for the two transfer ellipses of (b),  
 d) Calculate the magnitudes of  $\mathbf{v}_1$  and  $\mathbf{v}_1^{\#}$ ,  
 e) calculate  $p$  and  $\tilde{p}$  (in au) along with  $e$  and  $\tilde{e}$ .  
 f) for the two ellipses, perform the graphical construction for  $\alpha$  and  $\beta$  described in the text.

- 4.3\* Determine the expression (4.34) for  $t_p$ , the transfer time on a parabolic orbit between points  $P_1$  and  $P_2$ . Start with Eq. (4.25) for an elliptic orbit and proceed to the limit as  $a \rightarrow \infty$ . Be sure to account for the two cases  $\theta \leq \pi$  and  $\theta > \pi$ .
- 4.4 Calculate the sum of  $t_F$  for  $\theta < \pi$  and  $t_F^{\#}$  for  $\theta > \pi$  for a given elliptic orbit and interpret your result using Fig. 4.4.
- 4.5 Show that  $p_m = 2(s - r_1)(s - r_2)/c = r_1 r_2 (1 - \cos \theta)/c$ .
- 4.6 Specialize the expressions for  $\alpha$ ,  $\beta$ , and  $t_2 - t_1$  to the case of a *circular* arc of radius  $r_c$  and transfer angle  $\theta$ .
- 4.7 For the case  $r_1 = r_2 \equiv r_o$  and an arbitrary transfer angle  $\theta$ ,
  - a) Construct the locus of the focus.
  - b) For a value of  $a$  equal to  $r_o$  determine the values of  $e$  and  $\tilde{e}$  and the corresponding values of  $p$  and  $\tilde{p}$ .
- 4.8 Determine the terminal velocity vectors  $\mathbf{v}_1$  and  $\mathbf{v}_2$  [Eqs. (4.36) and (4.39)] for a parabolic orbit. Accomplish this by evaluating the variables  $A$  and  $B$  in Eqs. (4.37a) and (4.37b) in the limit as  $a \rightarrow \infty$ .

## 5

# Rocket Dynamics

## 5.1 Introduction

Beside gravity, the other major force that acts on a spacecraft is rocket thrust. There are a variety of types of rocket engines, typically categorized as either high- or low-thrust engines based on the magnitude of the thrust acceleration compared to the local gravitational acceleration. High-thrust engines can provide thrust acceleration magnitudes significantly higher than the local gravitational acceleration, while the value is typically several orders of magnitude less than gravity for a low-thrust engine. With either type of engine, the rocket mass is not constant, but decreases due to the fact that some mass is expelled out of the rocket nozzle to provide thrust, which is the reaction force in the opposite direction.

## 5.2 The Rocket Equation

In order to obtain the equation of motion for a system having a time-varying mass, one utilizes the fundamental form of Newton's Second Law, namely that the time rate of change of linear momentum relative to an inertial frame of reference is equal to the net external force acting on the system.

For the case of the rocket shown in Fig. 5.1 the variable  $m$  is the instantaneous mass of the rocket and  $\mathbf{v}$  is the vector velocity of the center of mass of the rocket relative to an inertially fixed point labeled  $O$ .

The vector  $\mathbf{c}$  is the effective exhaust velocity of the engine. The exhaust velocity is the velocity of the expelled particles *relative to the rocket*; the adjective *effective* implies that the effect of any nonzero exit pressure at the nozzle has been compensated for, in the case of a chemical rocket engine. This will be explained later.

For convenience, let us define the mass flow rate  $b$  as

$$b = -\dot{m} \geq 0 \quad (5.1)$$

where  $\dot{m}$  is negative because the mass  $m$  of the rocket is decreasing with time as the engine is operating.